Light Metals 2014
Edited by: John Grandfield
TMS (The Minerals, Metals & Materials Society), 2014

GRAIN REFINEMENT AND NANOPARTICLE DISPERSION USING TRAVELING MAGNETIC FIELD

Mariano Garrido[1], Yves Fautrelle[1], Laurent Davoust[1],
Valdis Bojarevics[2], Koulis Pericleous[2], Mustafa Megahed[3], Ole Koeser[4]

[1]SIMAP-EPM, BP 75, 38402 Saint Martin d'Héres, France
[2]University of Greenwich, Park Row, London, SE10 9LS,UK
[3]ESI Engineering System International, Kruppstraße 82, 45145 Essen, Germany
Calcom ESI SA, Parc Scientifique EPFL / PSE-A ,1015 Lausanne, Switzerland

Keywords: Grain refinement, metal matrix composites, traveling magnetic field, electromagnetic mixing

Abstract

Improvement in the mechanical properties of different alloys can be achieved by the reduction of the crystallite (grain) size and promoting an equiaxed microstructure. This can be achieved by the use of micro- and nano-particles as grain refiners, effectively dispersed within the material. Simap lab has developed a Bridgman furnace equipped with a traveling magnetic field (TMF) with the objective to produce grain refinement in alloys. TMF is utilized to stir molten material and disperse the particles within the matrix material. In addition, TMF-induced stirring will increment the nucleation points due to the breaking of the dendritic arms at the solidification front, and homogenize the temperature of the liquid metal, which also helps to produce equiaxed dendrites. Experiments carried out, supported with numerical simulations performed by University of Greenwich and ESI Group, will demonstrate the benefits obtained from the use of TMF combined with an accurate temperature control.

Introduction

The size of the grains forming the structure of a material has a great influence on its mechanical properties. The type of grain is also influential in the resistance to hot tearing and the cast rate of ingots made of this material [1]. Usually a metal with no treatment would solidify in a coarse columnar grain structure [2, 3]. In order to enhance the mechanical properties of the material, the transition from columnar to equiaxed grains (CET) should be promoted and the grain size reduced. The use of inoculants such as TiB_2 microparticles as grain refiners has shown to very efficient [4, 5]. The introduction and distribution of the particles inside the material represents always a challenge especially when the particle size is decreased. For this task, different methods have been developed such as mechanical stirring, pulse magnetic fields or ultrasounds. One of the main advantages obtained using magnetic fields to refine materials is the completely contactless influence on the liquid metal. In the case of a traveling magnetic field, the capacity of directing the flow and control its intensity by modifying the electric current and its frequency, should be added. These capacities could be developed to produce a correct distribution of the inoculant particles within the matrix material and to control macrosegregation. In addition, TMF can be used to increase the nucleation points which will enhance the reduction of grain size in the alloy [6, 7], and to homogenize the temperature of the melt. The near – zero gradient field will prevent the growth of cellular dendrites while helping to produce equiaxed ones [8, 9]. Melting light metal alloys (Al, Mg, etc) in the presence of electromagnetic (EM) field can help to diffuse inclusions of various sizes in the liquid volume or oppositely concentrate these on the surface of the melt. Barnard et al. [10] demonstrated experimentally that melting in a high frequency AC field indeed brings particles to selected locations on the surface of consequently solidified metallic sample. Bubbles and inclusions are observed to move selectively in the presence of EM field during steel casting [11]. Materials of special properties, like an increased concentration of additive particles near the surface, are produced in the presence of the imposed electromagnetic field [12]. Numerically the particle paths can be predicted [13, 14] accounting for the added electromagnetic force effects using the force proposed by Leenov & Kolin [15]. The electromagnetic force acts directly only on electrically conducting inclusions, however the electromagnetic force in the surrounding fluid creates a gradient of pressure giving additional integral force even on the non-conducting inclusions of various sizes and composition. The gravity induced buoyancy acts vertically, but the EM 'buoyancy' acts in the direction opposite to the EM force. In addition to this, the large scale electromagnetically driven flow circulation exerts a drag force, torque and shear which contributes to the particulate transport. This paper exposes the results obtained using a TMF of low intensity during the on melting of aluminum alloy A357 with TiB_2 microparticles with the purpose of grain refining. The experiments were supported by the numerical modeling of the crucible. The results obtained will be used to support future experiments in which nano-size particles will be used as grain refiners.

Experimental Procedures

Experiments were carried out using a Bridgman furnace equipped with a Bitter coil. The furnace VB2 (Vertical Bridgman 2 inches) manufactured by Cybestar is characterized by having two distant zones separated by a temperature gradient controlled area. The hot and cold zones are equipped with graphite resistors for heating. This Bitter coil provides a traveling magnetic field of 10 mT and frequency of 50 Hz. The phase shift is set as 0, 60, 120, 180, 240 and 300 degrees (Figure 6).

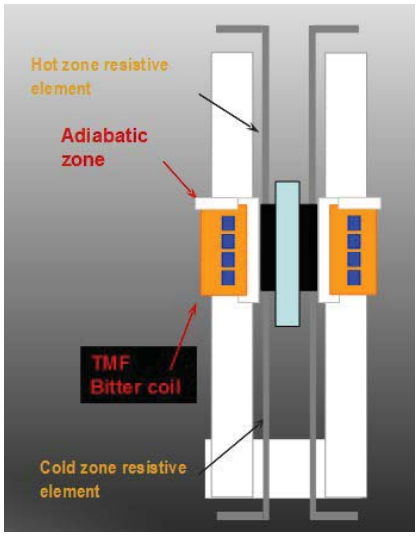

Figure 1. Scheme of the furnace.

The material selected to be refined was aluminum alloy A357. This aluminum alloy is commonly used in casting of aerospace structures. Table 1 shows its chemical composition.

Table I. Composition of aluminum alloy A357.

Element	Al	Mg	Si	Ti	Be
Weight %	92.25	0.60	7.00	0.15	0.005

TiB_2 microparticles were selected to be mixed with aluminum alloy A357. Their density and average diameter are 4.52 g/cm^3 and 8.6 µm respectively. The amount of material to be melted is calculated to obtain a cylindrical specimen with a diameter of 5 cm and a height of 15 cm. The final weight of the specimen is 730 g, 0.85 % of it is provided by the microparticles. The microparticles and aluminum alloy A357 are introduced at the same time inside a crucible made of quartz. For this purpose, a pile of aluminum plates containing TiB_2 microparticles was made (Figure 2). In order to avoid the agglomeration of the particles and enhance their dispersion; the plates contain only a fine layer of microparticles inside a shallow hole made in one their sides.

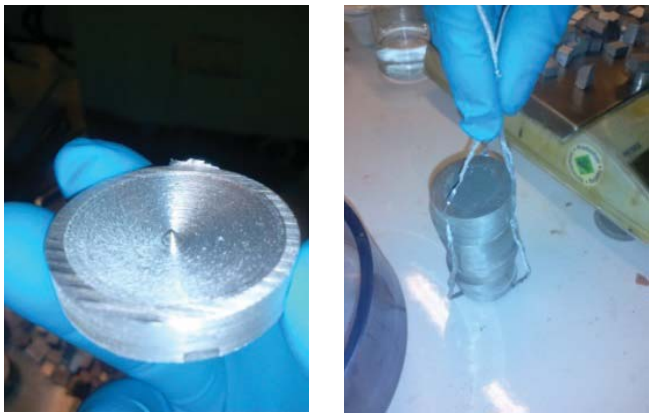

(a) (b)

Figure 2. Standard aluminum plate (a); Plates filled with TiB_2 prepared to be introduced inside the crucible (b).

The aluminum plates containing particles are covered with more material cut into small pieces to attain the required weight (Figure 3).

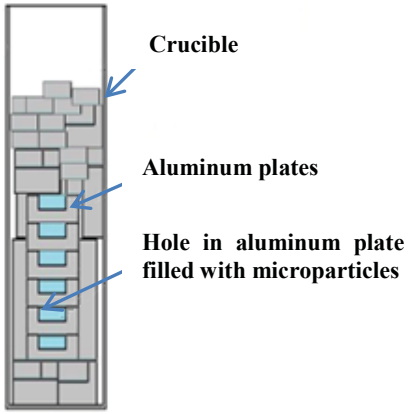

Figure 3. Crucible cross section.

Aluminum has a very high reactivity with the oxygen and readily forms aluminum oxide. In order to avoid an oxide layer over the surface of the crucible, the furnace is subjected to vacuum conditions, approximately 10^{-3} mbar at the beginning of the experiment. Afterwards, an open cycle of argon flow of 2.3 l / min is maintained during the total time of the experiment. The pressure inside the furnace is maintained in this way at 1200 mbar.

Figure 4 shows the empty crucible inside the Bitter coil area. The dimensions of the specimen are adapted to the dimensions of the coil. Therefore, all the material in the crucible will be under the influence of the magnetic field.

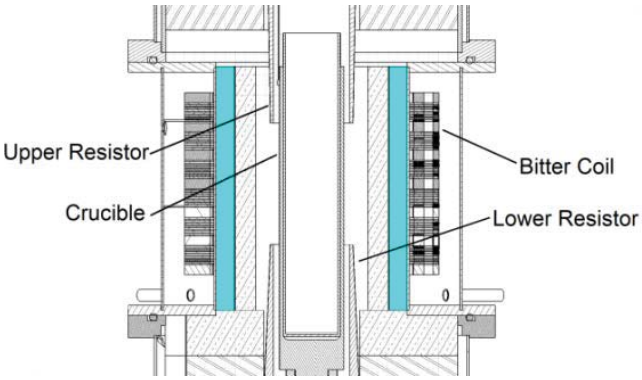

Figure 4. Cross section area of the furnace in which can be seen the Bitter coil and crucible.

The crucible filled with aluminum alloy A357 was heated using upper and lower resistors to a temperature of 800° C and 700 °C respectively. A gradient along the crucible of 660 K/m was obtained. These temperatures were kept during 1.5 h. Electromagnetic stirring started when the temperatures were attained. Upwards and downwards TMF was alternated every 10 minutes and set to upwards direction during the cooling period until the solidification of the material. Rapid cooling would enhance the reduction of the grain size [16]. Therefore, the cooling rate selected was 0.25 K/s for all the experiments.

The Mathematical Model And Results

The mathematical basis of the present model is the time-dependent Navier-Stokes and continuity equations for an incompressible fluid, and the thermal energy conservation equations with the Joule heating term for the fluid and solid zones of the metal charge [17]. The turbulent viscosity and the effective thermal diffusivity is the subject of the turbulence model accounting for the EM effects. The numerical solution of the coupled equations is obtained using the pseudo-spectral collocation method, employing the continuous co-ordinate transformation for the shape tracking. The time-dependent fluid flow problem is set with appropriate boundary conditions: at the free surface of the liquid metal the normal hydrodynamic stress is compensated by the surface tension, whilst at the solid walls the no-slip condition is applied to the velocity wherever there is contact at any given time. The free surface contact position moves as determined by the force balance and the kinematic conditions. During the melting or solidification, the solid-liquid interface is traced automatically as the solidus temperature surface $T = T_S$ moves with the coupled effects of the solid fraction-modified specific heat function.

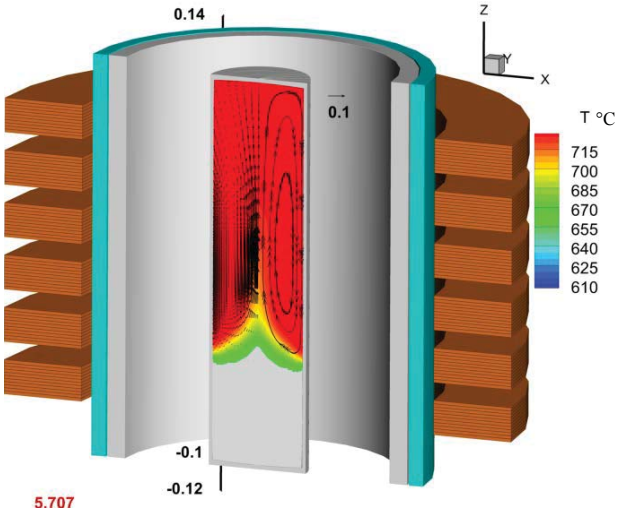

Figure 5. The computational model results for the flow in the experimental furnace using 50 Hz 2*3-phase downward traveling magnetic field.

The temperature field corresponds to the thermally insulating side wall, the linearly decreasing in time hot top/cold bottom condition. The EM mixing and the additive particle distribution can be investigated using advanced numerical models combining the time dependent EM fields, developing flow fields, the moving free surface and solidification front. The present paper gives an insight to the numerical modeling applied to the specific AC EM mixing experiment where the liquid aluminum is solidified in a controlled temperature gradient imposed mostly by the external graphite heaters. The EM mixing is achieved by a specially designed Bitter type coil arranged in separate sections with a prescribed phase shift. The device is shown in the Figure 4 and the numerical model with a computed velocity field in the Figure 5.

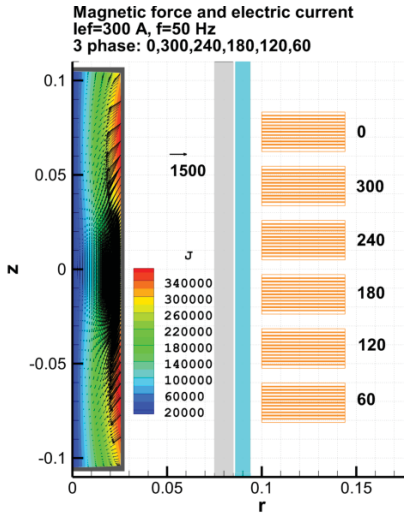

Figure 6. The computed EM force (time average) in the experimental furnace using 50 Hz 2*3-phase downward travelling magnetic field.

The AC phase shift permits to create the traveling magnetic field either upward or downward (Figure 6 shows the time average EM force distribution) , which permits a variety of the mixing patterns affecting the impact onto the solidification front and various scenarios of the particle motion.

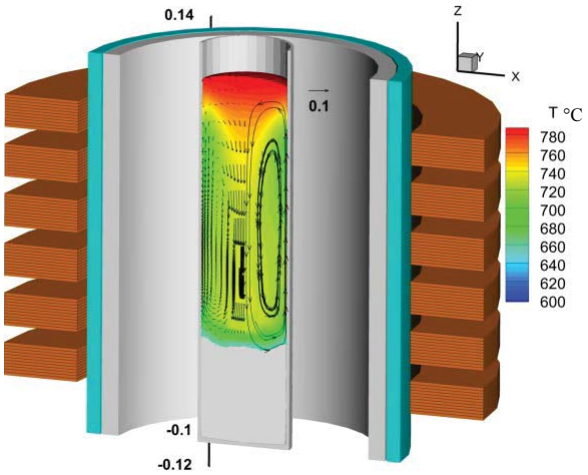

Figure 7. The upward traveling magnetic field generated flow in the experimental furnace using 50 Hz 2*3-phase.

The particles of micro to nano-size can be added at desired locations in order to follow their paths and the concentration, eventually affecting their distribution in the gradually solidified metal ingot. Larger particles (> 10 μm) are affected by the buoyancy and the direct EM force effects, while smaller size particles follow closely the fluid flow pattern, only deviating in the regions of the higher EM force density and being entrapped when reaching the solidification front. The choice of flow pattern ensures the desired distribution of the particles. The downward traveling field created flow (Figure 8) leads to enhanced particle concentration at the top part of the melt (Figure 7), thus delaying or even preventing the additive supply to the solidification front.

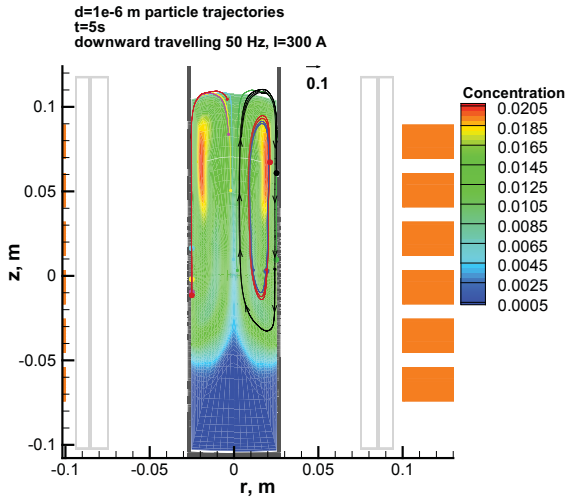

Figure 8. The particle (1 micron size) paths and concentration after 5 s mixing in the downward traveling magnetic field generated flow as in Figure 5.

The upward EM field favors the fast entrapment of the particles (Figure 9) at the bottom solidification front (compare to the Figure 7).

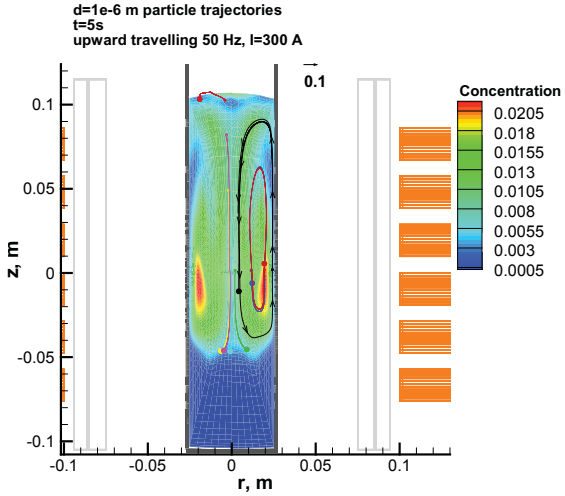

Figure 9. The particle (1 micron size) paths and concentration after 5 s mixing in the upward traveling magnetic field generated flow as in Figure 7.

The results presented are preliminary and a full experimental verification is needed. However, they served to choose the optimum settings for the experiments carried out. The model showed areas in which the magnetic field is more intense and the best flow direction for the dispersion. The highest intensity of the magnetic field was found on the middle of the Bitter coil area. In consequence, the particles would be more effectively dispersed if they are positioned there at the beginning of the experiment. The crucible can be moved up or down thanks to a piston situated on its base. Therefore, in order to obtain the maximum stirring of the material, it was moved in both directions during few minutes of the experiment to position all the liquid metal inside the area with the maximum magnetic field.

Results and Discussions

Particle Dispersion

The microscopic study of the specimens revealed an apparently good dispersion of the particles (Figure 10 and 11) along the specimen length. Agglomeration and settling can easily occur due to the difference in density between aluminum and TiB_2. The images obtained from the analysis of material from the lower part of the crucible showed no signs of agglomeration.

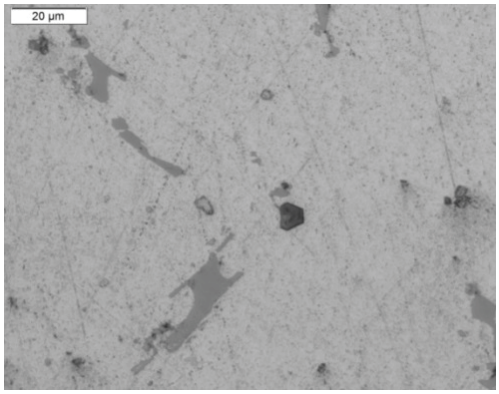

Figure 10. A single microparticle embedded in aluminum matrix found near the center area on the lower part of the specimen.

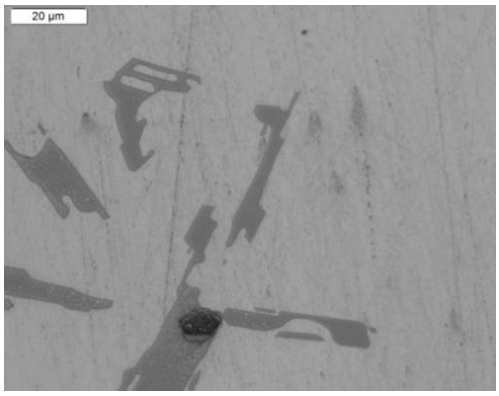

Figure 11. A hole left by a TiB_2 particle found on the upper part of the specimen. The extraction of the particles could have been the result of the polishing performed on the samples.

The upper part of the specimen showed different results. The number of particles found during the first optical inspection was similar than on the lower part. Single particles such as the one shown in Figure 12 were found, but also signs of possible TiB_2 agglomerates (Figure 13). The characterization of the specimens is still in process and the number of particles will be determined accurately in future work.

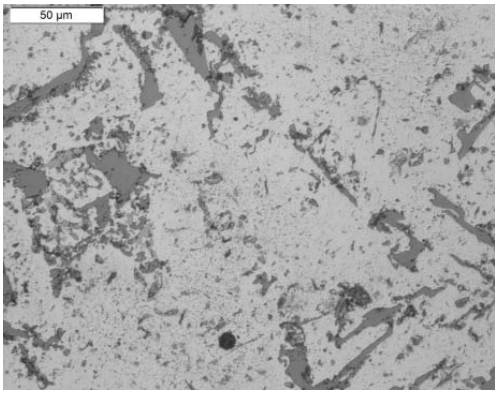

Figure 12. Isolated TiB_2 particle found in the upper part of the specimen.

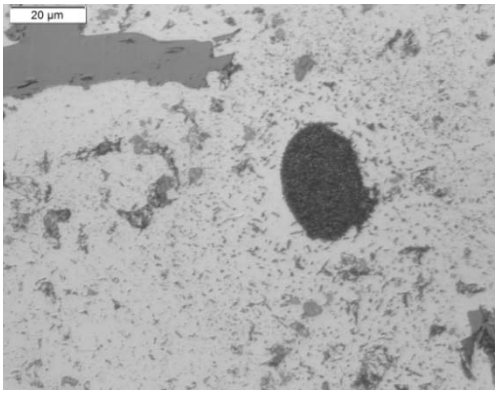

Figure 13. Agglomeration of TiB_2 particles found in the upper part of the specimen.

Microstructures

The following images were taken from samples of the lower part of the specimen at distances of less than 1 cm from the crucible wall. The images show equiaxial dendrites grown from refining particles (Figure 14) and also some signs of porosity (Figure 15).

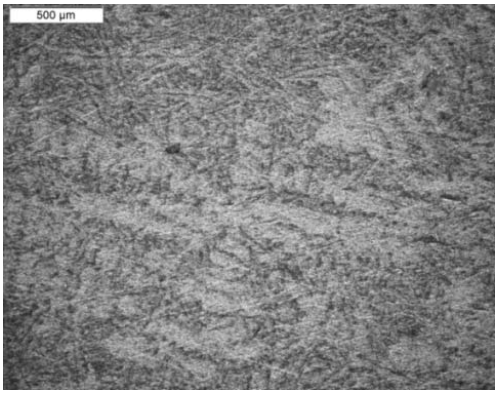

Figure 14. Equiaxial dendrite. The refining particle can be seen positioned in its center.

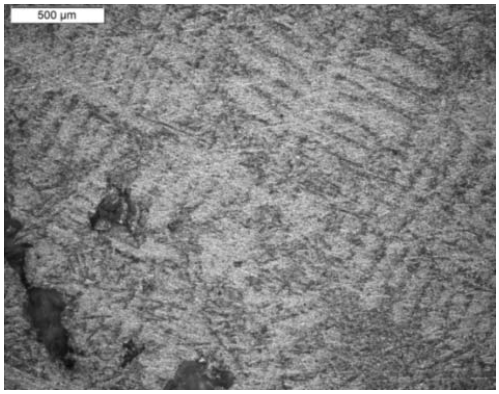

Figure 15. Equiaxial dendrite and some signs of porosity.

Refining

The following pictures were taken from samples taken from the upper part of the specimen. There are clear signs of refining in the sample of aluminum A357 in which TiB_2 microparticles were introduced (Figure 16). The microstructure obtained in Aluminum alloy A357 without grain refiner but under the same experimental conditions can be seen in Figure 17.

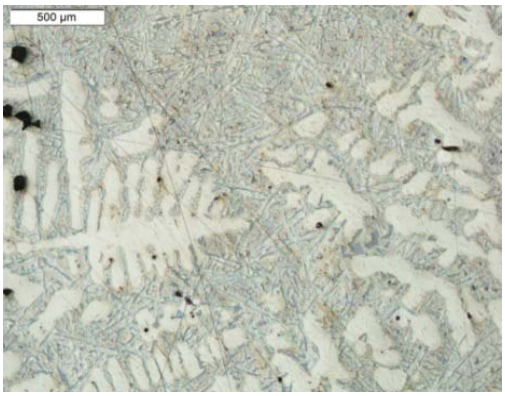

Figure 16. Aluminum alloy 357 refined with TiB_2 microparticles. It can be observed the refined particles of silicon and also some primary dendrites which are typical of non-equilibrium solidification.

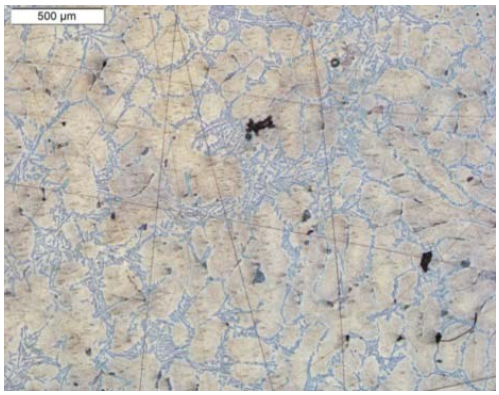

Figure 17. Aluminum alloy 357 stirred without grain refiner.

Conclusions

Intense mixing can be achieved using both upwards and downwards traveling magnetic field. The velocity magnitudes will grow proportional to the current magnitude in the coil. The melt front shape is strongly affected by the flow direction and the type of side wall thermal conditions. The particle paths and concentration can be optimized to the desired outcome manipulating the EM field. The combined use of grain refiner and low intensity traveling magnetic field has shown positive results in the refining of the material. The initial results showed some signs of agglomeration but an average good dispersion of the particles. No signs of particles rejected from the matrix material were found. Further studies to determine accurately the grain size; the map of the macrosegregation and the average position of the particles will determine the grade of effectiveness of the process. The success of these experiments is the first step to proceed with the introduction of smaller particles in the nano metric scale.

References

1. Carlos E.Suarez, Grain refining of Pure Aluminium. Light Metals 2012, (TMS, The Minerals & Materials Society, 2012), 96.

2. R. Kumar, "Br. Foundryman", 1972, 65, (2), 56–72.

3. M. C. Flemings: Solidification processing, (New York, McGraw-Hill, 1974) 41–344.

4. Greer AL,Bunn AM,Tronche A, Evans PV, Bristow DJ. Acta Mater (2000);48-2823.

5. Spittle JA, Int J. Cast Metal Res (2006), 19-210.

6. D.G McCartney, "Grain Refining of Aluminium and Its Alloys using Inoculants", *International Materials Reviews*,1989, no.5:247-260.

7. Alcoa Report, ''New Process for Grain Refinement of Aluminium,'' (DOE Project Final Report, Contract No. DE-FC07-98ID13665, 2000).

8. C. Vives, "Hydrodynamic, thermal and crystallographical effects of an electromagnetically driven rotating flow in solidifying aluminium alloys". *Int. J. Heat Mass Transfer*, 33 (1990), 2585-2598.

9. J.K. Roplekar, J.A. Dantzig, "A study of solidification with a rotating magnetic field". *Int. J. Cast Metals Res*, 14, (2001), 79-95.

10. L. Barnard, R.F. Brooks, P.N. Quested and K.C. Mills, Evaluation of alloy cleanness using cold crucible melting" *Ironmaking and Steelmaking*, 20, (1993), 344-349.

11.J.W.Haverkort, T.W.J. Peeters. Magnetohydrodynamic effects on insulating bubbles and inclusions in the continuous casting of steel". *Metallurgical and Materials Transactions*, 41 (B) (2010), 1240-1246.

12. S. Taniguchi, A. Kikuchi: "Removal of Nonmetallic Inclusion from Liquid Metal by AC-Electromagnetic Force", *Proceedings of the 3rd International Symposium on Electromagnetic Processing of Materials ISIJ, Nagoya*, (2000), 315-320.

13. D. Leenov and A. Kolin, "*Journ. Chem. Phys*", 22 (4) (1954), 683-688.

14. T. Toh, H. Yamamura, "Kinetics Evaluation of Inclusions Removal During Levitation Melting of Steel in Cold Crucible". *ISIJ International*, 47 (11) (2007), 1625-1632.
.

15. V. Bojarevics, K. Pericleous and R. Brooks. "Dynamic Model for Metal Cleanness Evaluation by Melting in Cold Crucible", *Metallurgical and Materials Transactions*, 40 (3) (2009), 328 – 336.

16. Joseph R. Davis, *Aluminum and aluminum alloys*, Illustrated edition, (ASM International, 1993), 98.

17. V. Bojarevics, R.A. Harding, K. Pericleous and M. Wickins, '*Metallurgical and Materials Transactions*', 35 (B) (2004), 785-803.

Acknowledgments

The authors acknowledge financial support from the ExoMet Project (co-funded by the European Commission (contract FP7-NMP3-LA-2012-280421), by the European Space Agency and by the individual partner organissations.